

Synthesis of MgO/ZnO hetero-epitaxial whiskers using chemical vapor deposition operated under atmospheric pressure

H. SAITOH*, Y. OKADA, S. OHSHIO

*Department of Chemistry, Nagaoka University of Technology,
Kamitomioka, Nagaoka, Niigata 940-2188, Japan
E-mail: hts@nagaokaut.ac.jp*

A chemical-vapor-deposition (CVD) technique operated under atmospheric pressure is available to synthesize metal oxide crystals with various morphologies. This CVD technique provides highly supersaturating conditions that induce morphological instability of growing crystallites. In this study, the metal oxide material with rock salt structure was selected to confirm the possibility of whisker growth of the cubic system crystal. The MgO whiskers grew epitaxially on the single crystalline substrate of (0001) sapphire under appropriate conditions. The MgO whiskers were also formed epitaxially on the top of the ZnO whiskers. The unique whisker with the MgO/ZnO hetero-junction was successfully obtained. © 2002 Kluwer Academic Publishers

1. Introduction

Synthesis of the crystalline phase of metal oxides has been attempted using a chemical-vapor-deposition (CVD) technique operated under atmospheric pressure [1, 2]. The feature of this technique is to possess an ability to synthesize various forms of the metal oxide crystal with widely changing in the degree of supersaturation on the reaction process. Under low supersaturation conditions, the growth rate of the metal oxide crystallites is usually low, producing continuous polycrystalline films. With increasing the degree of supersaturation, morphological instability of the crystal occurs; that is, the surface of the continuous films becomes rough. The growth rate also increases with the degree of supersaturation. The resulting film consists of the aggregation of the columnar crystals. When further high degree of supersaturation is given to the reaction process, the columnar crystals are clearly separated each other. This type of structure often forms the aggregation of the crystalline whiskers. This technique is absolutely unique due to its ability to provide wide variation of morphologies of the metal oxide crystal.

The CVD technique operated under atmospheric pressure uses β -diketone or metal-alkoxides as the source material. For example, when Zn 2,4-pentanedionate was used as the source, ZnO homogeneous polycrystalline films and ZnO whiskers grew on the solid-state substrate at low and high supersaturating conditions of the precursor, respectively. On the substrate of single crystalline Si, the whiskers grew nearly normal to the substrate within a deviation of $\pm 5^\circ$. On the other hand, on the substrate of single crystalline

(0001) sapphire, the whiskers grew epitaxially [3, 4]. As the epitaxial relationship is ZnO $[\bar{1}010](0001) \parallel$ sapphire $[\bar{1}2\bar{1}0](0001)$, ZnO whiskers crowd together and align to $\langle 0001 \rangle$ direction. The conductive whiskers of aluminum-doped ZnO, Al:ZnO, are also obtained with a combination of Al- and Zn-complexes [5].

As mentioned above, the CVD method operated under atmospheric pressure is available for crystal growth with morphological instabilities. Highly supersaturating condition that is favorable for growth of ZnO whiskers may promote growth of various types of metal oxide whiskers. The present work focuses on aspects of synthesis of the MgO whiskers with rock salt structure. There are two reasons why we select MgO for whisker growth. The first reason is that cubic system may have disadvantageous for whisker growth due to its isotropic structure. Therefore, it is thought to be difficult to promote anisotropic growth of the isotropic crystals. Success in whisker growth of cubic system implies that the possibility of whisker growth with all crystal systems exists. The second reason is that the MgO/ZnO hetero-junction is necessary for design of the fundamental photo-electronic devices. For example, it was reported that the metal oxide semiconductor junction between the aggregations of n-type ZnO microcrystals and p-type MgO microcrystals would be a candidate for ultraviolet solid-state lasers [6]. We expect that the aggregation of MgO/ZnO hetero-whiskers also to be an important candidate.

In this study, epitaxial growth of MgO whiskers was attempted on the (0001) sapphire substrate followed by successful synthesis of the MgO/ZnO hetero-junction whiskers. The morphology and epitaxial relationship

* Author to whom all correspondence should be addressed.

between ZnO and MgO whiskers will be described and discussed.

2. Experimental

Single crystalline (0001) sapphire substrates were obtained from Dowa Co., and polished with a mis-cut value of within 0.1° . The substrate was cut into a size of $5 \times 10 \times 0.5 \text{ mm}^3$ and then ultrasonically cleaned sequentially with trichloroethane, acetone, and methanol. After treatment, the single crystal was washed with deionized water for 30 minutes. On the (0001) sapphire substrate, MgO, having a lattice constant of $a_0 = 0.42112 \text{ nm}$ at a temperature of 25°C , grows along (111) orientation. Although there is a relatively large difference on the three-dimensional arrangement between hexagonal system and cubic system, in-plane arrangement between (0001) sapphire and (111) MgO is nearly same. Regarding atomic configuration, the position of every 12th oxide ion of MgO overlaps with the position of every 13th oxide ion of sapphire with a mismatch of less than 9%.

MgO and ZnO whiskers were prepared using an atmospheric CVD apparatus as shown in Fig. 1 that was previously employed in obtaining epitaxial anatase films [4], with titanium tetra-isopropoxide as the source complex. The reactant, $\text{Mg}(\text{C}_5\text{H}_7\text{O}_2)_2$ and/or $\text{Zn}(\text{C}_5\text{H}_7\text{O}_2)_2$ (Soekawa Chemical Co., quoted purity of 99.9%), was loaded into a vaporizer and vaporized using an electric heater. The inside temperature of the vaporizer measured using a *K*-type thermocouple is defined as the vaporizing temperature. The reactant vapor was first carried by nitrogen gas flowing at a rate of $1.2\text{--}1.5 \text{ dm}^3/\text{min}$ and then sprayed from the metallic nozzle directly onto the single crystalline (0001) sapphire substrate mounted on the electric heater. The surface temperature measured using the *K*-type thermocouple is defined as the substrate temperature. The reactant vapor was immediately decomposed by thermal energy from the substrate heater to form whiskers. The deposition duration of MgO and ZnO crystallites was maintained for 100 minutes for each experiment using a metallic shutter placed below the nozzle. The substrate was heated to $500\text{--}650^\circ\text{C}$ using the electric heater. The distance between the nozzle and the substrate was maintained at 15 mm throughout the experiments. X-ray diffraction analysis (using M03XHF, Mac Science Co.) was conducted to reveal the crystal structure, the growth direction and the epitaxial relation-

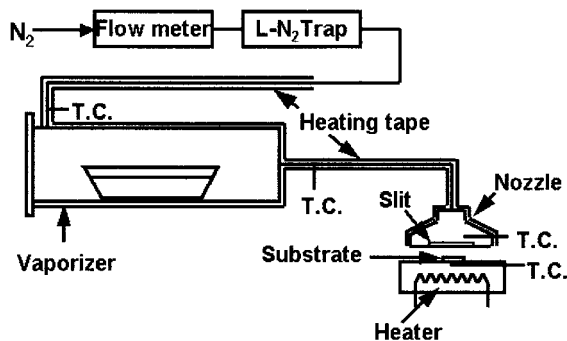


Figure 1 Schematic diagram of CVD apparatus operated under atmospheric pressure.

ship between the whisker and the substrate. The surface and cross-sectional morphology of the whiskers was observed by scanning electron microscopy (SEM, using JEOL, JSM T-300). The growth rate of the film or the whisker was determined by the thickness or length observed using cross-sectional observation.

3. Results and discussion

3.1. MgO epitaxial whiskers on sapphire

A first series of growths were performed at a substrate temperature of 600°C and the vaporizing temperatures ranging from 220°C to 240°C in 5°C steps. The MgO whiskers grew on the substrate at the vaporizing temperatures more than 225°C . As supersaturation of the precursor generated from source material in the reaction process is dependent upon the vaporizing temperature, the dependency of morphological instability on the vaporizing temperature should be observed. The morphology of the metal oxide whisker was also sensitive to the substrate temperature. A second series of growths were performed at the substrate temperatures ranging from 550°C to 640°C . Fig. 2a–d show SEM micrographs of the MgO samples grown at a vaporizing temperature of 240°C . While the homogenous film of MgO was obtained at the substrate temperatures less than 550°C , whiskers grew on the substrate temperatures more than 600°C . One of conditions for whisker growth requires presence of a precursor suction with high reaction rate on the specific crystalline face [4].

When the reaction rate on the specific face is dependent upon the temperatures in the reaction process with a positive correlation, the growth rate should increase with the substrate temperature. Fig. 3 indicates the growth rate and the diameter of the MgO crystals observed in Fig. 2. The growth rate was dependent upon the substrate temperature with the positive correlation. At a substrate temperature of 640°C , a growth rate of 10.6 nm/s was obtained as a maximum value. The diameter of the whisker also increased from $3.8 \mu\text{m}$ to $9.0 \mu\text{m}$, when the substrate temperature increased from 600°C to 640°C . These results suggest that the growth rate increases not only along vertical axis but also along horizontal axis with the temperature rise. However, since it is thought that only the growth front of the whisker becomes the precursor suction, growth of the diameter occurs only at the whisker tip.

Fig. 2d was obtained during the SEM observation along the surface normal of the sample grown at a substrate temperature of 600°C . The crystalline particles with about $2\text{--}5 \mu\text{m}$ in size created relatively small space at the grain boundary. The hexagonal edge direction of each crystallite was completely aligned. This type of morphology often suggests that the possibility of that crystals grow epitaxially on the substrate is relatively high. The top view shows that the MgO crystallites possess two distinct heteroepitaxial arrangements with the sapphire lattice. The reason for the coexistence of two directional images will be discussed later.

The result of SEM observation suggested that the whiskers grew epitaxially. The epitaxial relationship between MgO and sapphire single crystals along to in-plane and out-of-plane was examined. Fig. 4 shows the

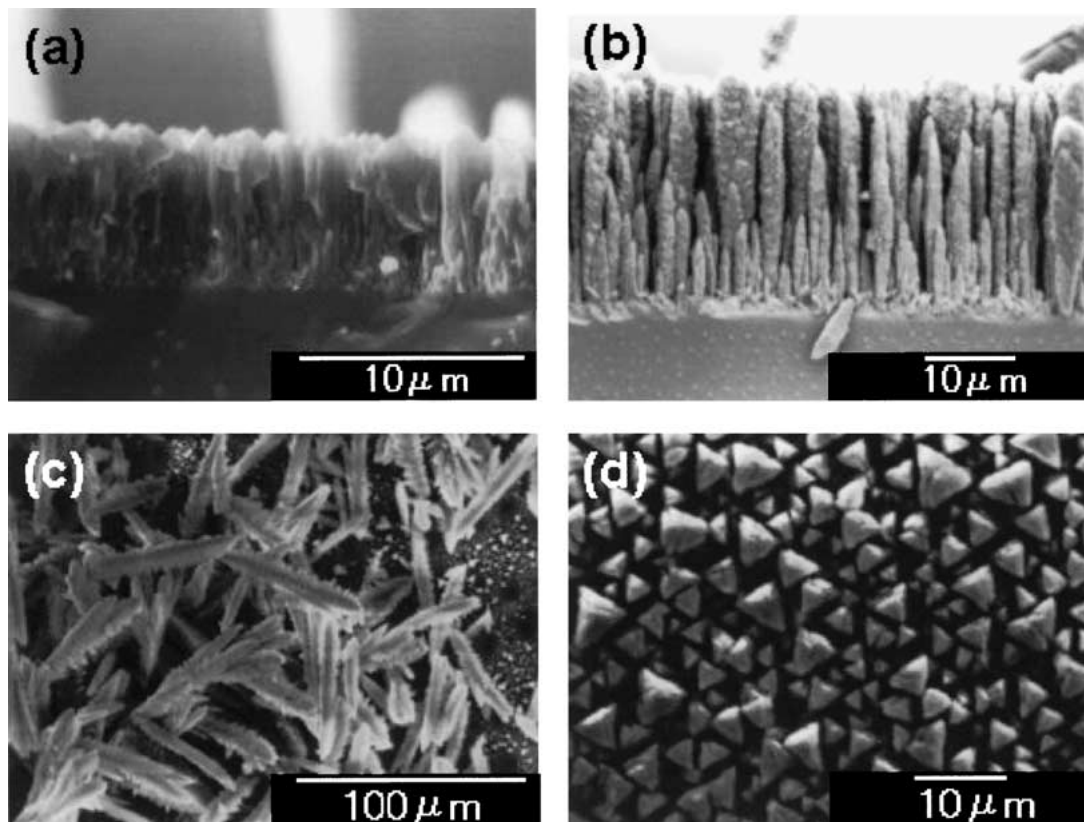


Figure 2 SEM micrographs of MgO crystallites: (a), (b) cross-sectional view of the crystallites grown at the substrate temperatures of 550°C and 600°C; (c) top view of the broken whiskers grown at the substrate temperature of 640°C; and (d) top view of the whiskers grown at the substrate temperature of 600°C.

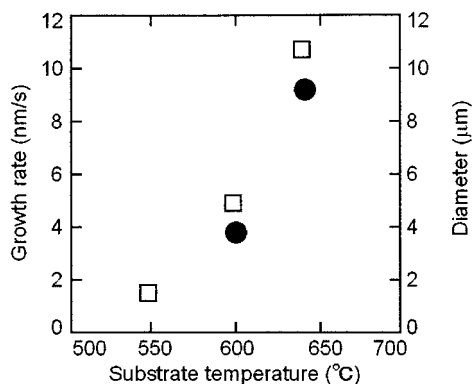


Figure 3 Growth rate (□) of the MgO crystallites and diameter (●) of the MgO whiskers.

2θ X-ray diffraction pattern of the sample formed at various substrate temperatures. The most major change is the growth direction of MgO crystals. From the sample deposited at the substrate temperature of 550°C, only (200) diffraction line was observed, implying the preferential orientation toward (100) direction. On the other hand, only (111) diffraction line was seen from the sample deposited at the substrate temperature of 600°C – 640°C, suggesting that the MgO crystals oriented toward (111). Although the substrate temperature gives a strongly influence on the preferential growth direction, no morphological instability was occurred.

To understand the degree of preferential orientation, rocking curve measurement was performed. Although the full width half maximum (FWHM) value of the sample grown at the substrate temperature of 550°C was 0.64°, those of the samples obtained at 600°C and

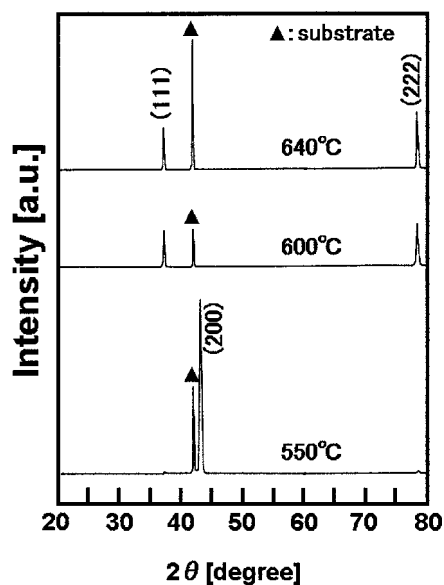


Figure 4 2θ X-ray diffraction patterns of MgO crystallites grown on *c*-cut sapphire.

640°C were 0.86° and 0.96°. These values were slightly larger than that of the epitaxial ZnO whiskers, 0.47°, implying that perturbation of the growth direction from the normal axis is slightly large.

In-plane orientation was also evaluated. First, that of the single crystalline *c*-cut sapphire was examined. The sapphire crystal was rotated from the standard angle $\phi = 0$, then ω scan was measured each angle ϕ as shown in Fig. 5. As sapphire has (11 $\bar{2}$ 9) plane showing six-fold symmetry, ω scan indicates two diffraction lines ($\bar{1}\bar{1}29$) and (11 $\bar{2}$ 9). For example, at the standard angle $\phi = 0$,

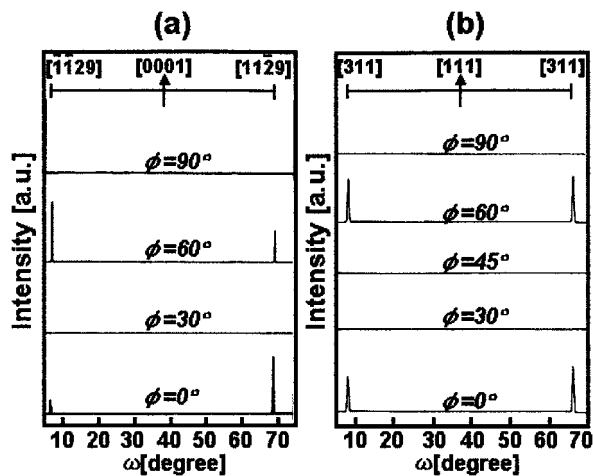


Figure 5 ϕ - ω X-ray rocking curves of (a) *c*-cut sapphire and (b) MgO crystallites grown on *c*-cut sapphire.

($\bar{1}\bar{1}29$) and ($11\bar{2}9$) planes that incline $\pm 31.3^\circ$ from the *c* axis should be obtained at $\omega = 7.6^\circ$ and 69.9° . X-ray diffraction shows the results expected above. Similar patterns were also obtained at $\phi = 1/3n\pi$, where *n* is integer. For (111) oriented MgO crystal, similar measurement was performed as shown in Fig. 5b, where that the standard angle $\phi = 0$ is coincides to that in Fig. 5a. The (311) plane of MgO has (311) peaks showing three-fold symmetry. Therefore patterns should be obtained every $\phi = 2/3n\pi$. For example, MgO (311) appears $\omega = 66.8^\circ$ at $\phi = 0$ followed by the next appearance at $\phi = 2/3\pi$. In addition, MgO (113) or (131) line may be observed at $\omega = 7.8^\circ$ when the crystal is rotated by $\phi = 1/3\pi$, and therefore next appearance is located at $\phi = \pi$. However, in Fig. 5b, MgO (311), and (131) or (113) diffraction lines were observed at both $\omega = 7.8^\circ$ and $\omega = 66.8^\circ$ every $1/3n\pi$.

A reason why two diffraction lines appear on both $\omega = 7.8^\circ$ and $\omega = 66.8^\circ$ at the same ϕ is explained using the atomic configuration as shown in Fig. 6. In Fig. 2, two types of triangle images aligned toward two different directions were observed. With considering the crystallographical relationship obtained from the results in Fig. 5, it is found that a possibility of presence of two crystalline directions along in-plane configuration exists. Because the angle difference between two crystalline directions is just π , two diffraction patterns are superimposed together, resulting that the pattern is

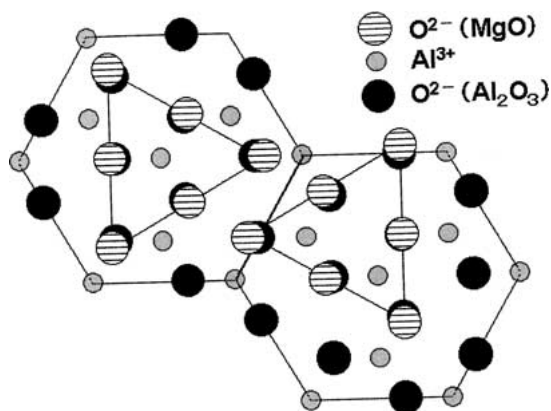


Figure 6 Atomic configuration of MgO crystallites epitaxially grown on *c*-cut sapphire.

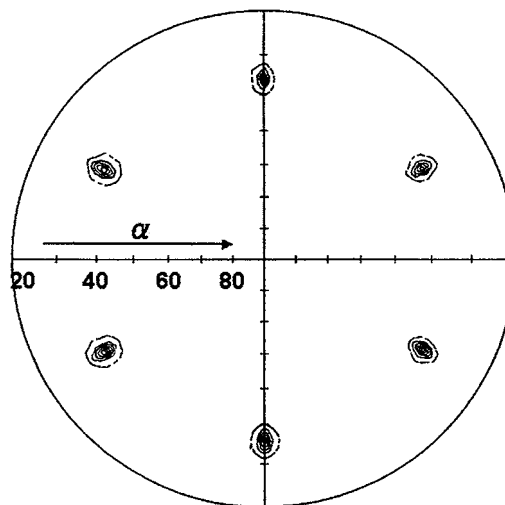


Figure 7 Pole figure of MgO crystallites grown on *c*-cut sapphire.

equal to that with the six-fold symmetry. Consequently two (311) and (131) or (113) diffraction lines appear at every $\phi = 1/3n\pi$.

For the MgO (200) pole figure, 2θ is set to 42.9° , therefore the poles in the stereograms reveal the tilt and azimuthal angles for all MgO (200) planes present in the sample. The pole figure displaying the pole positions in the equiangular Wulff net projection for a sample grown along to (111) direction at the substrate temperature of 600°C is shown in Fig. 7. The six prominent poles at a tilt angle, $\alpha = 35.3^\circ$ are the MgO (200) poles from (111) MgO crystals, since the angle between MgO (111) and MgO (200) is 54.7° . This shows that most of the sample has a MgO (111) orientation. Since MgO has three-fold symmetry about [111] direction, there are six prominent poles from MgO crystals having two in-plane orientations. To establish the heteroepitaxial relationship, we examine the *c*-cut sapphire stereogram. Here we observe poles with six-fold symmetry at the angle of 58.7° , the angle between sapphire (0001) and ($11\bar{2}9$). The sapphire ($11\bar{2}9$) poles lie at precisely the same azimuthal angles as the MgO (200). This establishes the heteroepitaxial arrangement of the MgO (111) crystals as $\text{MgO}[111] \parallel \text{Al}_2\text{O}_3[0001]$ and $\text{MgO}[11\bar{2}] \parallel \text{Al}_2\text{O}_3[11\bar{2}0]$.

3.2. MgO/ZnO whiskers

ZnO whiskers were epitaxially synthesized on the single crystalline *c*-cut sapphire. The perturbation of the *c*-axis was held in $\pm 0.5^\circ$ from the normal axis. On the epitaxial ZnO whiskers, crystal growth of MgO was attempted. While only a small amount of MgO crystal grew on the tip of the ZnO whisker at the vaporizing temperature of 220°C , MgO whiskers grew on them at the temperature of 240°C .

Fig. 8a shows the cross-sectional image of the MgO/ZnO whiskers deposited at a vaporizing temperature of 240°C and a substrate temperature of 600°C . Fig. 8b indicates the top view of the MgO/ZnO whiskers, showing that the MgO whiskers possess two distinct heteroepitaxial arrangements with the ZnO whiskers. Crystalline particles with about $2\text{--}5 \mu\text{m}$ in size created space at the grain boundary. The hexagonal edge direction of each crystallite was completely

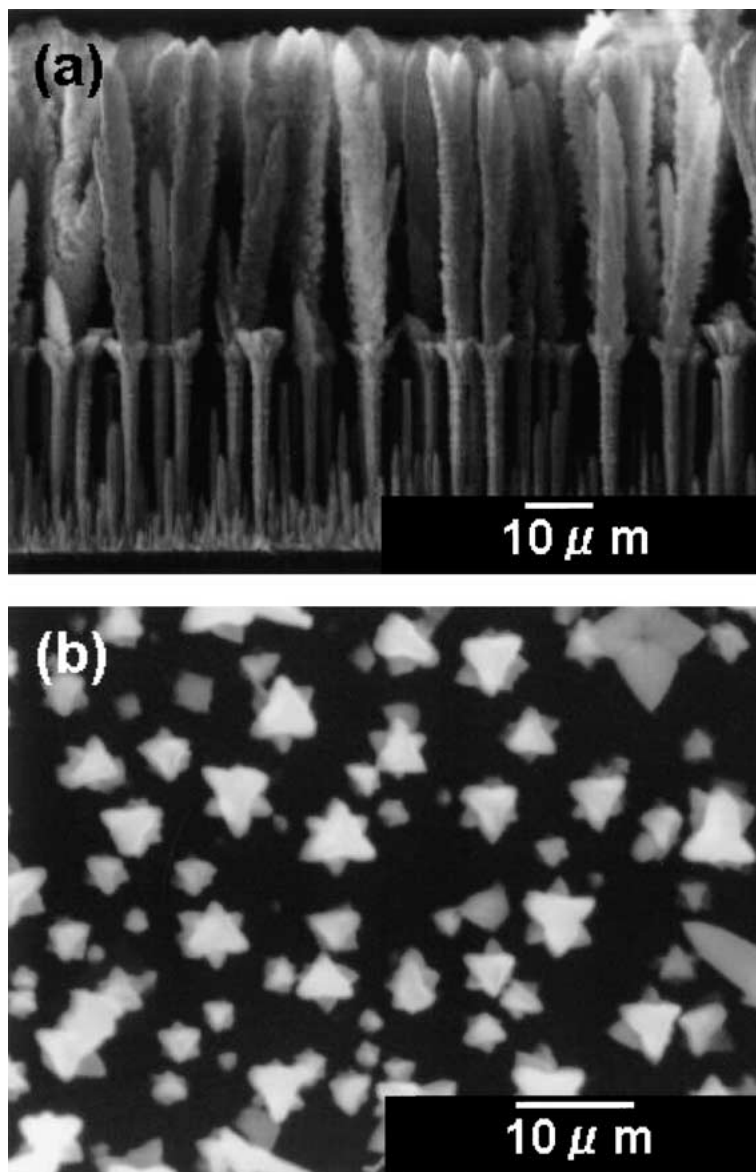


Figure 8 SEM micrographs of MgO crystallites grown on ZnO epitaxial whiskers: (a) cross-sectional view and (b) top view of the crystallites.

aligned. This type of morphology often suggests that the possibility of that crystals grow epitaxially on the substrate is relatively high. Here, we call it MgO/ZnO heterowhiskers.

Only four diffraction lines, ZnO(0002), ZnO(0004), MgO(111) and MgO(200), were obtained from the 2θ measurement of the MgO/ZnO hetero-whiskers as shown in Fig. 9, indicating ZnO[0001] and MgO[111] are aligned along the normal to the surface of the substrate. For the MgO(200) pole figure, 2θ is set to 42.9° , therefore the poles in the stereograms reveal the tilt and azimuthal angles for all MgO(200) planes present in the sample. The pole figure displaying the pole positions in the equiangular Wulff net projection for a sample grown along to (111) direction at the substrate temperature of 600°C is shown in Fig. 10. Three types of diffraction line were observed: a broad line at $\alpha = 90^\circ$, relatively weak six-fold lines at $\alpha = 47^\circ$ and relatively strong six-fold lines at $\alpha = 35^\circ$. The first line is attributable to the MgO(200) diffraction that is role out from the epitaxial relationship ZnO(0001)∥MgO(111). At the initial stage of the whisker growth, X-ray diffraction revealed that both MgO(111) and (100) oriented

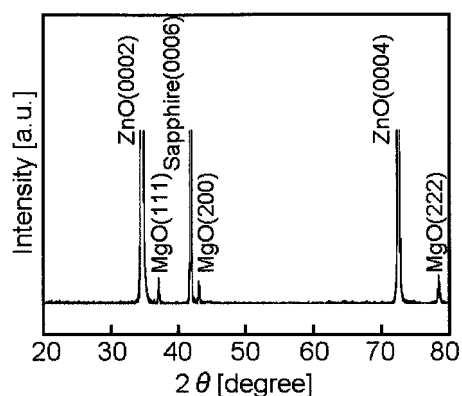


Figure 9 2θ X-ray diffraction pattern of the MgO/ZnO hetero-whiskers.

whiskers nucleated. However only MgO(111) whisker can finally be grown due to the faster growth rate than that of MgO(100) crystallite. The second diffraction lines at $\alpha = 47^\circ$ is examined. This α angle of the diffraction is attributable to the (10 $\bar{1}$ 2) reflection of the ZnO(0001) whisker appeared at the theoretical α angle 47.2° , indicating perfect six-fold in-plane alignment of the ZnO whiskers. Finally, diffraction lines at

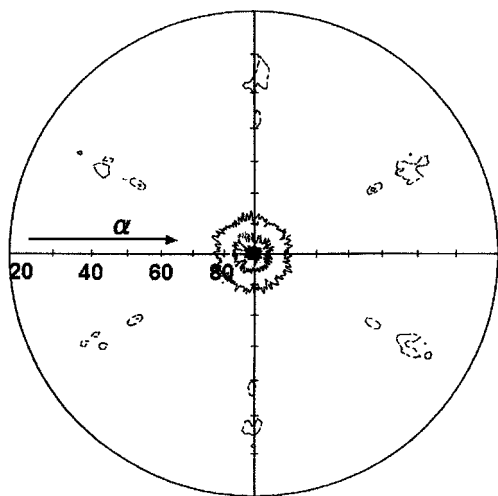


Figure 10 Pole figure of MgO crystallites grown on epitaxial ZnO whiskers.

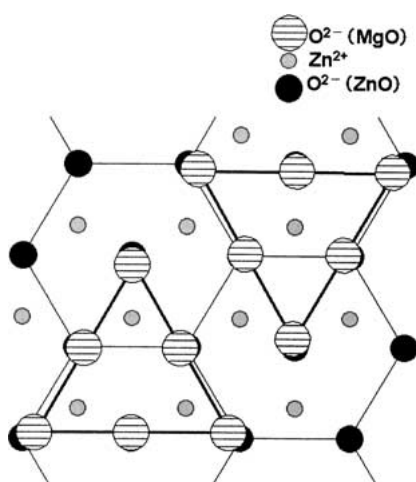


Figure 11 Atomic configuration of MgO crystallites epitaxially grown on ZnO lattice.

$\alpha = 35^\circ$ is examined. This α angle of the diffraction is attributable to the (200) reflection of the MgO(111) whisker appeared at the theoretical α angle of 35.5° , indicating perfect six-fold in-plane alignment (three-fold multiplied by two) of the MgO whiskers. The ZnO (10 $\bar{1}$ 2) poles lie at precisely the same azimuthal angles as the MgO(200). This establishes the heteroepitaxial arrangement of the MgO(111) crystals as MgO[111]||ZnO[0001] and MgO[110]||ZnO[11 $\bar{2}$ 0] or MgO[11 $\bar{2}$]||ZnO[10 $\bar{1}$ 0]. Fig. 11 shows the atomic con-

figuration of the MgO(111) lattice grown epitaxially on the ZnO(0001) lattice. Regarding atomic configuration, the position of every 12th oxide ion of MgO overlaps with the position of every 11th oxide ion of ZnO with a mismatch of less than 9%.

4. Conclusion

First, MgO whiskers were synthesized epitaxially on the single crystalline *c*-cut sapphire using the atmospheric CVD apparatus. The sapphire (11 $\bar{2}$ 9) poles lie at precisely the same azimuthal angles as the MgO(200). This establishes the heteroepitaxial arrangement of MgO(111) crystals as MgO[111]||Al₂O₃[0001] and MgO[11 $\bar{2}$]||Al₂O₃[11 $\bar{2}$ 0] or MgO[110]||Al₂O₃[10 $\bar{1}$ 0]. Next, MgO whiskers were also synthesized epitaxially on the epitaxial ZnO whiskers using the same technique. The ZnO (10 $\bar{1}$ 2) poles lie at precisely the same azimuthal angles as the MgO(200). This establishes the heteroepitaxial arrangement of the MgO(111) crystals as MgO[111]||ZnO[0001] and MgO[110]||ZnO[11 $\bar{2}$ 0] or MgO[11 $\bar{2}$]||ZnO[10 $\bar{1}$ 0].

Acknowledgment

This work was supported by a Grant-in-Aid for Scientific Research from the Ministry of Education, Science, Culture, under Contract No. 11450247.

References

1. N. TANAKA, S. OHSHIO and H. SAITOH, *J. Ceram. Soc. Jpn.* **105** (1997) 551.
2. S. TOKITA, N. TANAKA and H. SAITOH, *Jpn. J. Appl. Phys.* **39** (2000) L169.
3. M. SATOH, N. TANAKA, Y. UEDA, S. OHSHIO and H. SAITOH, *ibid.* **38** (1999) L586.
4. H. SAITOH, M. SATOH, N. TANAKA, Y. UEDA and S. OHSHIO, *ibid.* **38** (1999) 6873.
5. H. SAITOH, Y. NAMIOKA, H. SUGATA and S. OHSHIO, *ibid.* **40** (2001) 6024.
6. A. OHTOMO, T. MAKINO, K. TAMURA, Y. MATSUMOTO, Y. SEGAWA, Z. TANG, G. K. L. WONG, H. KOINUMA and M. KAWASAKI, *Proc. SPIE* v3941 (2000) (Society of Photo-Optical Instrumentation Engineers, Bellingham, WA, USA) p. 70.

Received 6 November 2001
and accepted 18 July 2002